BMC Oral Health

RESEARCH

Open Access

Baicalin attenuates LPS-induced periodontal inflammation response by inhibiting autophagy

Yifan Cheng[1,2,3], Ming Jiang[1,2,3], Xu Qin[1,2,3], Jing Mao[1,2,3*], Yan Liu[4*] and Guangxun Zhu[1,2,3*]

Abstract

Background Periodontal disease causes gradual damage to the periodontal ligament and alveolar bone, ultimately resulting in tooth loss. This condition This condition results from the intricate interaction between bacterial infections and the host's inflammatory responses, driving disease progression. Autophagy, an essential process for cellular balance under stress, plays a vital role in the response to periodontal pathogens. Baicalin (BA), a flavonoid extracted from *Scutellaria baicalensis*, is recognized for its potent anti-inflammatory effects. However, its influence on autophagy in periodontal health is not fully characterized, representing a vital gap in therapeutic understanding.

Purpose This study investigates the therapeutic potential of BA in periodontal disease by examining its regulatory effects on autophagy and inflammation in PDLCs.

Methods Periodontal ligament cells (PDLCs) were exposed to various concentrations of BA, and cell proliferation was measured using the CCK-8 assay. Anti-inflammatory responses were analyzed by quantitative real-time PCR (qRT-PCR) and enzyme-linked immunosorbent assay (ELISA). Autophagy levels were quantified using immunofluorescence, transmission electron microscopy (TEM), and Western blotting. To identify potential targets of BA, an integrated approach combining network pharmacology and RNA sequencing (RNA-Seq) was employed. These analyses were subsequently validated using qRT-PCR, molecular docking and dynamics simulations.

Results BA significantly reduced lipopolysaccharide (LPS)-induced inflammatory responses in PDLCs, as evidenced by a decrease in the levels of interleukin (IL)-1β and IL-6. RNA-Seq analysis indicated that these effects were associated with autophagy-related processes. Notably, BA decreased Beclin-1 levels, reduced the LC3BII/I ratio, diminished LC3B protein staining, and decreased the number of autophagosomes. Furthermore, BA triggered the activation of the PI3K/AKT/mTOR pathway, demonstrated by the increased phosphorylation of these proteins.

Conclusion BA acts as a protective agent against LPS-induced periodontal inflammation by modulating autophagy, positioning it as a promising candidate for future periodontal therapies.

*Correspondence:
Jing Mao
maojing@hust.edu.cn
Yan Liu
orthoyan@bjmu.edu.cn
Guangxun Zhu
zhuguangxun@163.com

Full list of author information is available at the end of the article

One-Sentence Summary

Baicalin attenuates LPS-induced periodontal inflammation by inhibiting autophagy and activating the PI3K/AKT/mTOR signaling pathway in periodontal ligament cells.

Keywords Baicalin, Periodontal disease, Autophagy, Inflammation, Transcriptomic sequencing analysis, Network Pharmacology

Introduction

Periodontal disease, a common oral condition, is mainly initiated by pathogens in dental plaque biofilms, including *Porphyromonas gingivalis* (*P. gingivalis*), resulting in persistent inflammation and progressive damage to periodontal tissue [1]. Specifically, *P. gingivalis* activates host immune cells through the secretion of lipopolysaccharide (LPS), which triggers the production of inflammatory cytokines, including interleukin (IL)-6, IL-1β and tumor necrosis factor alpha (TNF-α). These cytokines not only sustain and exacerbate the inflammatory response but also contribute to the degradation of bone resorption and extracellular matrix [2]. Autophagy, a crucial cellular process for maintaining homeostasis and responding to cellular stress, is key in modulating these inflammatory processes [3]. It facilitates the elimination of damaged organelles and proteins, thus protecting cells from ongoing damage caused by the inflammatory environment. However, chronic bacterial stimulation can lead to an abnormal increase in autophagic activity, which, if excessive, may result in cellular dysfunction and further exacerbate cell injury and tissue destruction [4].

This review comprehensively elaborated on the essential involvement of autophagy in periodontal disease, including regulating periodontal infection, modulating inflammatory responses, influencing periodontal tissue remodeling and cell function, managing endoplasmic reticulum stress, and affecting disease progression particularly in high-risk factors such as smoking [5]. Recent studies have shown that autophagy is a key player in the inflammatory and repair processes of periodontal disease. For instance, LPS from *P. gingivalis* activates the PI3K/AKT/mTOR pathway, promoting autophagy in human gingival fibroblasts (HGFs) and regulating inflammation [6]. Hyperglycemia exacerbated the production of IL-1β and induced pyroptosis in macrophages exposed to periodontal pathogens, with autophagy modulating this response by targeting the ROS-inflammasome axis, thus mitigating the progression of diabetes associated periodontitis [7]. Additionally, CKIP-1 has been shown to promote inflammation in periodontal soft tissues caused by *P. gingivalis* by suppressing autophagy, both in vitro and in vivo [8]. PINK1-mediated mitophagy maintains mitochondrial homeostasis, preventing bone loss and playing a crucial role in tissue repair during periodontal disease [9]. Moreover, autophagy influences various cell death pathways, including cuproptosis. Copper chelation using tetrathiomolybdate (TTM) has been shown to alleviate periodontal inflammation by inhibiting cuproptosis while enhancing autophagic flux [10]. Therefore, regulating the balance of autophagic activity is of potential significance in the treatment of periodontal disease.

Baicalin (BA), a flavonoid extracted from the traditional Chinese herb *Scutellaria baicalensis*, has been well-documented for its profound anti-inflammatory, antioxidative, and immunomodulatory properties in the management of inflammatory diseases [11]. Our previous studies have established that BA significantly reduces the release of matrix metalloproteinase (MMP)-8 from polymorphonuclear neutrophils (PMNs) triggered by IL-8, and suppresses MMP-1 expression induced by IL-1β at both mRNA and protein levels [12, 13]. These findings elucidate the mechanism through which BA modulates periodontal inflammatory responses. Further, a comprehensive review has underscored BA's efficacy in mitigating bone loss, collagen degradation, and inflammatory infiltration in periodontal tissues affected by periodontitis, reinforcing its potential for periodontal therapy [14]. Recent studies further underscore the broad therapeutic potential of BA in modulating autophagy across various disease models. In a hypertensive heart injury model, BA mitigated angiotensin II-induced cardiac damage by cell death and autophagic processes through the AMPK/mTOR pathway [15]. Similarly, in an acute graft-versus-host disease (aGVHD) model, BA improved survival and reduced pathological scores by regulating autophagy [16]. In a rat model of status epilepticus (SE), BA alleviated LiCl-pilocarpine-induced hippocampal damage through autophagy activation [17]. Moreover, BA attenuated hyperglycemia-induced embryonic cardiovascular malformations by decreasing excessive reactive oxygen species (ROS) and modulating autophagy [18]. BA also suppressed autophagy triggered by the H3N2 influenza virus in A549 and Ana-1 cells [19]. Lastly, in *Mycoplasma gallisepticum* (*M. gallisepticum*) infection models, BA mitigated inflammation and apoptosis via autophagic modulation [20]. These findings indicate that the capacity of BA to regulate autophagy extends beyond periodontal disease and holds broad therapeutic potential. However, despite its established effects in conditions like osteoarthritis (OA), rheumatoid arthritis (RA) and allergic rhinitis (AR) [21–23], the specific role of BA in modulating autophagy within periodontal disease models, along

with its underlying mechanisms, remains underexplored, presenting a critical gap in current research. Beyond its effectiveness in various animal models, clinical studies have highlighted BA's broad therapeutic potential. BA has significantly improved lipid profiles and reduced inflammation markers in patients with cardiovascular diseases and RA [24]. Moreover, BA has shown effectiveness in managing acute lymphoblastic leukemia by regulating immune responses and inducing apoptosis in white blood cells [25]. It has also outperformed standard medications in treating coughs caused by acute tracheobronchitis [26] and reduced postoperative pain after dental surgeries [27], demonstrating its anti-inflammatory capabilities. When used alongside non-surgical periodontal therapy, BA not only improves periodontal health indicators but also notably decreases inflammatory mediators [28]. This supports its potential as a non-invasive treatment option for periodontal diseases.

This study utilizes an in vitro inflammation model constructed with *Pg*-LPS (*P. gingivalis*-Lipopolysaccharide) to investigate how BA modulates autophagy and related signaling pathways in PDLCs, providing new clinical insights and strategies for targeted drug development aimed at combating periodontal disease. Additionally, it provides a theoretical basis for advancing the development of unique plant resources and high-activity plant components in China, underscoring their significant clinical relevance.

Methods

Network Pharmacology

The PubChem database was searched to obtain the 2D molecular structures, chemical formulas, and standard SMILES representations. The name of BA was input into the TCMSP, HIT 2.0, and the Swiss Target Prediction plat to identify its potential target proteins. The target name was used to locate the associated target gene, with the species filter set to Homo sapiens in the UniProt database. Data on target genes related to periodontal disease were gathered from databases such as GeneCards, OMIM, and DisGeNET (v7.0). Cytoscape 3.6.1 was used to construct both the drug-protein-target and disease-drug-target networks. Overlapping targets between the disease and the drug were identified and visualized using a Venn diagram.

Transcriptomic sequencing analysis

Total RNA was isolated from the hPDLCs using the RNA Extraction Kit (Axygen, China) after treatment with either 0 μg/mL *Pg*-LPS, 1 μg/mL *Pg*-LPS, or 40 μM BA in the presence of *Pg*-LPS for 12 h. After RNA extraction, PCR amplification was conducted, and the resulting products were sequenced using the PE150 sequencing strategy on the Illumina HiSeq 2500 high-throughput platform.

Cell culture and treatment

Healthy premolars were extracted from orthodontic patients aged 18–25 years (mean age 21.5 years) with ethical approval from the Tongji Hospital Ethics Committee. Written informed consent was obtained from all participants. Periodontal ligament tissues were aseptically scraped from the middle third of the tooth root, minced, and enzymatically digested with collagenase I (3 mg/mL, Biofroxx, Germany) and dispase II (4 mg/mL, Biofroxx, Germany) at 37 °C for 90 min. The digested suspension was filtered, centrifuged, and resuspended in α-MEM (Gibco, USA) supplemented with 10% fetal bovine serum and 1% penicillin/streptomycin. Cells were cultured at 37 °C with 5% CO_2, and the third and fifth generations were used for experiments. Immunofluorescence confirmed mesenchymal identity by vimentin expression and the absence of cytokeratin, excluding epithelial contamination. For treatment, hPDLCs were exposed to *Pg*-LPS (1 μg/mL, Invitrogen, USA) and various concentrations of BA (MCE, USA) for 12 h. To modulate the PI3K/AKT pathway, cells were pretreated with LY294002 (20 μM), a PI3K/AKT inhibitor, or 740Y-P (20 μM), a PI3K/AKT activator, before LPS treatment.

Cell counting kit-8 (CCK-8) assay

HPDLCs were incubated with increasing concentrations of BA (0, 1, 10, 20, 40, 80, 100 μM) for 12, 24 and 36 h, respectively. The CCK-8 assay (MCE, USA) was used to evaluate the effect of BA on cell viability, following the manufacturer's protocol. Absorbance was measured spectrophotometrically at 450 nm, and the percentage of viable cells was calculated as the ratio of absorbance relative to the control.

Quantitative real-time PCR (qRT-PCR)

Total RNA from hPDLCs was isolated using the RNA Extraction Kit (Axygen, China) and subsequently converted into cDNA with the Evo M-MLV Reverse Transcriptase Kit (Axygen, China). The obtained cDNA was analyzed by qRT-PCR on a LightCycler 96 system (Roche, China) using SYBR Green qPCR Master Mix (Axygen, China). Gene expression was quantified relative to GAPDH using the $2^{\Delta\Delta}$Ct method. Primer sequences for qRT-PCR are provided in supplementary Table S1.

Enzyme-linked immunosorbent assay (ELISA)

After the indicated treatments, the supernatant of cultured hPDLCs was stored at -80 °C until analysis. The levels of IL-6 and IL-1β in the supernatant were quantitatively assessed by an ELISA kit (Beyotime, China).

Western blotting analysis

Proteins were isolated from cultured PDLCs, and then concentrations were measured by a BCA protein assay kit (Beyotime, China). An equal quantity of protein from each sample was loaded onto SDS-PAGE gels and transferred to PVDF membranes. The membrane was incubated with TBST supplemented with 5% nonfat milk for blocking. PVDF membranes were left to incubate overnight with primary antibodies (complete information in supplementary Table S2). Protein bands were probed with horseradish peroxidase-conjugated secondary antibodies and analyzed using an ECL detection kit (MCE, USA).

Immunofluorescence

The cells were fixed with 4% paraformaldehyde for 10 min at room temperature. After permeabilization with 0.2% Triton X-100 for 10 min, they were blocked with 5% BSA for 30 min. Primary antibodies were incubated overnight at 4 °C (see in supplementary Table S2). The following day, cells were incubated with diluted fluorescent secondary antibodies for 1 h at 37 °C in the dark, followed by DAPI staining for 5 min. After washing, slides were mounted with glycerol and examined under a fluorescence microscope (LSM 880, Carl Zeiss). Fluorescence intensity of LC3B was quantified using ImageJ (Version 1.8).

Transmission electron microscopy (TEM)

The pretreated cells were collected and fixed with 2.5% glutaraldehyde overnight at 4 °C, subsequently post-fixation in 1% OsO_4 for 2 h at room temperature. The samples were dehydrated using increasing concentrations of ethanol and then embedded in epoxy resin. Thin sections were prepared and stained with uranyl acetate and lead citrate. Autophagosomes were visualized and measured using TEM in Tokyo, Japan.

Molecular Docking analysis and dynamics simulations

Molecular docking was performed to validate the target prediction results by docking selected active ingredients with hub genes. AutoDock Vina (Version 1.1.2) was used for docking the chemical components with targets, and results were visualized using PyMOL 2.3.2. To further evaluate the interactions between the compound and the protein target, molecular dynamics simulations of the baicalin-AKT complex were performed using GROMACS 2020.3.

Statistical analyses

Data analysis was performed using GraphPad Prism (Version 9.0.0). Data are presented as mean ± SD from at least three independent experiments. Comparisons between two groups were made using the student's t-test, while one-way ANOVA followed by Tukey's post-hoc test was used for multiple group comparisons. Differential gene expression in transcriptomic data was analyzed using DESeq2 or edgeR. Differentially expressed genes were selected based on FDR ≤ 0.05 and|log2FC| ≥ 1. Plots were generated with Hiplot Pro. Statistically significant differences ($P < 0.05$) are indicated by distinct lowercase letters.

Results

BA reduces LPS-induced inflammatory response in hPDLCs

Vimentin was positive and cytokeratin negative in isolated hPDLCs, confirming their fibroblast-like characteristics (Fig. 1A, supplementary Figure S1). The biosafety of BA in hPDLCs was assessed by the CCK-8 assay. At 100 μM, BA significantly inhibited cell growth, with a stronger effect at higher concentrations and longer exposure (Fig. 1B). Based on these results, concentrations of 20 μM (20BA), 40 μM (40BA), and 80 μM (80BA) were selected for further experiments. At 1 μg/mL LPS, a significant increase in IL-6 and IL-1β expression was observed (Fig. 1D-G), along with elevated levels of autophagy-related proteins LC3B and Beclin-1 (supplementary Figure S2A), guiding our choice of this concentration for subsequent studies. Similarly, at 12 h post-LPS treatment, a significant increase in LC3B and Beclin-1 expression was detected, supporting our selection of this time point for subsequent experiments (supplementary Figure S2C). BA treatment significantly attenuated the LPS-induced increases in inflammation-related gene expression (Fig. 1I and J) and reduced the secretion levels of these cytokines in the culture supernatants (Fig. 1K and L), with 40 μM demonstrating the most effective anti-inflammatory response. These findings demonstrate BA's potential to modulate inflammatory responses in periodontal disease, highlighting its anti-inflammatory properties.

BA attenuates LPS-induced inflammatory response through modulation of autophagy-related processes

RNA sequencing was used to investigate the possible molecular pathways through which BA exerts its effects in LPS-treated hPDLCs. A total of 34,494 were identified as differentially expressed. Specifically, in the CON/LPS group, 4,765 mRNAs were detected, with 1316 upregulated and 1192downregulated. In the LPS/LPS + 40BA group, 4,692 mRNAs were identified, with 510 upregulated and 636 downregulated (Fig. 2A–C). Venn diagrams were utilized to analyze the overlap between the CON/LPS and LPS/LPS + 40BA groups, revealing that 2,084 mRNAs were regulated by LPS and subsequently reversed by BA intervention (Fig. 2D). To further explore their functional implications, GO enrichment analyses were conducted, which showed that the genes reversed by BA were significantly associated with autophagy-related processes, including autophagy, regulation of

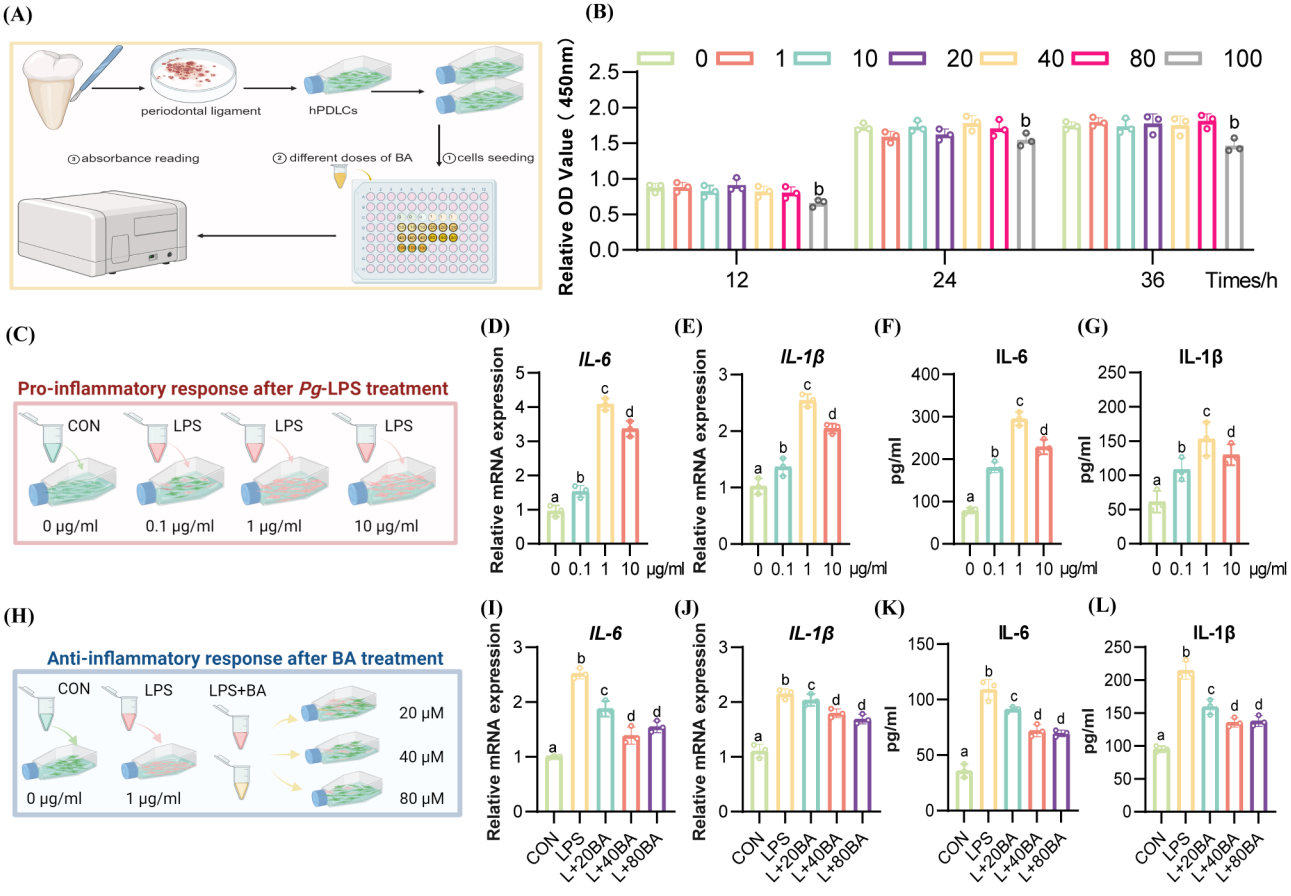

Fig. 1 BA reduces LPS-induced inflammatory response in hPDLCs. (**A**) Isolation of hPDLCs and cytotoxicity experimental procedure with different doses of BA (created with BioRender.com). (**B**) The impact of BA on hPDLCs' viability was evaluated using the CCK-8 method ($n=3$). (**C**) Experimental procedure for hPDLCs exposed to various concentrations of LPS (created with BioRender.com). (**D**-**G**) The levels of IL-6 and IL-1β in hPDLCs after 12 h of treatment with various LPS concentrations, measured by qRT-PCR (relative to GADPH, $n=3$) and ELISA ($n=3$). (**H**) Experimental procedure for hPDLCs exposed to various concentrations of BA (created with BioRender.com). (**I**-**L**) The levels of IL-6 and IL-1β in hPDLCs after 12 h of treatment with various BA concentrations, measured by qRT-PCR (relative to GADPH, $n=3$) and ELISA ($n=3$). Statistically significant differences ($P<0.05$) are indicated by distinct lowercase letters

autophagy, macroautophagy and negative regulation of autophagy (Fig. 2E). Collectively, the results indicate that the ability of BA to alleviate the LPS-induced inflammation is closely associated with autophagy-related mechanisms.

Network pharmacology and RNA-Seq analysis identified AKT1 as a target of BA in modulating hPDLCs autophagy

To provide a more accurate analysis, network pharmacology was employed to explore the involvement of BA in periodontal disease. A total of 185 herb targets and 1,138 disease targets were identified, with 64 overlapping genes (Fig. 3A). The protein-protein interaction (PPI) network highlighted AKT1 as a key target for BA in treating periodontal disease (Fig. 3B). Integration of omics and network pharmacology analyses revealed nine overlapping targets (Fig. 3C). To validate the findings from bioinformatics analysis, AKT1, DNMT1, HK1, NOD2, and JAK2 were randomly selected for further investigation. Heatmap analysis showed that AKT1, DNMT1, and HK1 were downregulated in the LPS group, while their levels notably elevated in the LPS + 40BA group. Conversely, NOD2 and JAK2 showed increased expression in the LPS group, but their levels were reduced in the LPS + 40BA group. (Fig. 3D). These findings were further confirmed by qRT-PCR for AKT1, DNMT1, HK1, NOD2, and JAK2 (Fig. 3E-I), with AKT1 showing the most significant change. Molecular docking simulations revealed that the AKT1-BA complex had a binding affinity of -6.0308 kcal/mol (Fig. 3J). Molecular dynamics simulations further supported the stability of the BA-AKT1 complex, as evidenced by RMSD equilibrium at 40 ns, reduced SASA and Rg values indicating structural compactness, and RMSF values below 7.5 Å (Fig. 3K-N). Hydrogen bond analysis revealed an average of 4.4 hydrogen bonds between BA and AKT1 (Fig. 3O). Given that AKT1 is a major regulator of autophagy, these results indicate that BA may modulate autophagy in hPDLCs through targeting AKT1.

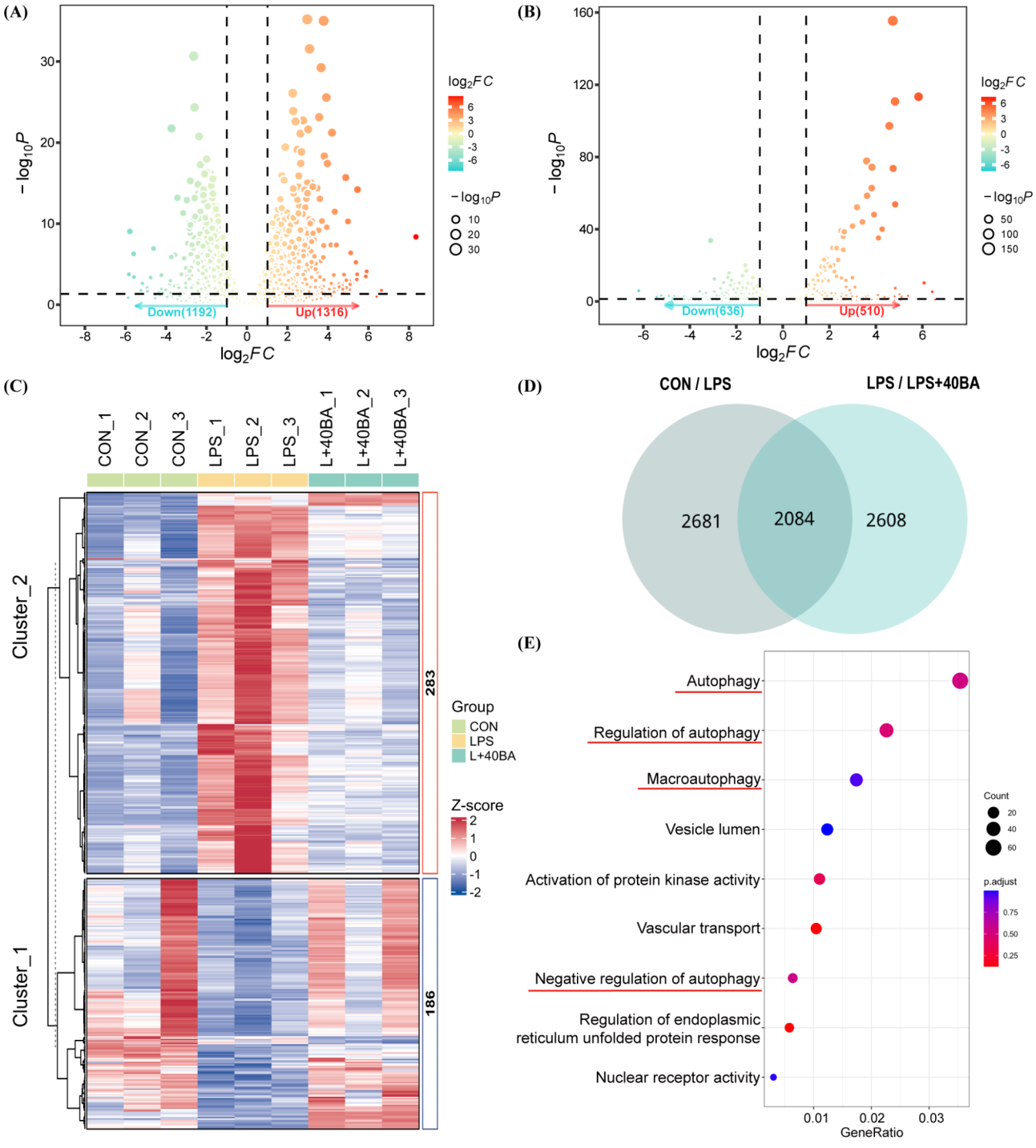

Fig. 2 RNA-Seq analysis of BA-reduced inflammatory response in LPS-stimulated hPDLCs. (**A**) Volcano plot showing the distribution of differentially expressed mRNAs in hPDLCs from the CON/LPS group ($n=3$). (**B**) Volcano plot representing the distribution of differentially expressed mRNAs in hPDLCs from the LPS/LPS + 40BA group ($n=3$). (**C**) Heatmap showing the cluster analysis of differentially expressed genes among the three groups. (**D**) Venn diagram depicting the overlap of mRNAs between the CON/LPS and LPS/LPS + 40BA groups. (**E**) Scatter plot showing GO enrichment analysis of genes with differential expression in hPDLCs

Inhibition of autophagy potentiated the anti-inflammatory effects of BA in hPDLCs

GSEA analysis indicated that genes upregulated in LPS-treated hPDLCs were notably associated with autophagy-related pathways (Fig. 4A), with higher levels of LC3B-II/ LC3B-I, and Beclin-1 observed (Fig. 4B and C, supplementary Figure S3). In contrast, BA treatment reduced the expression of autophagy-related genes

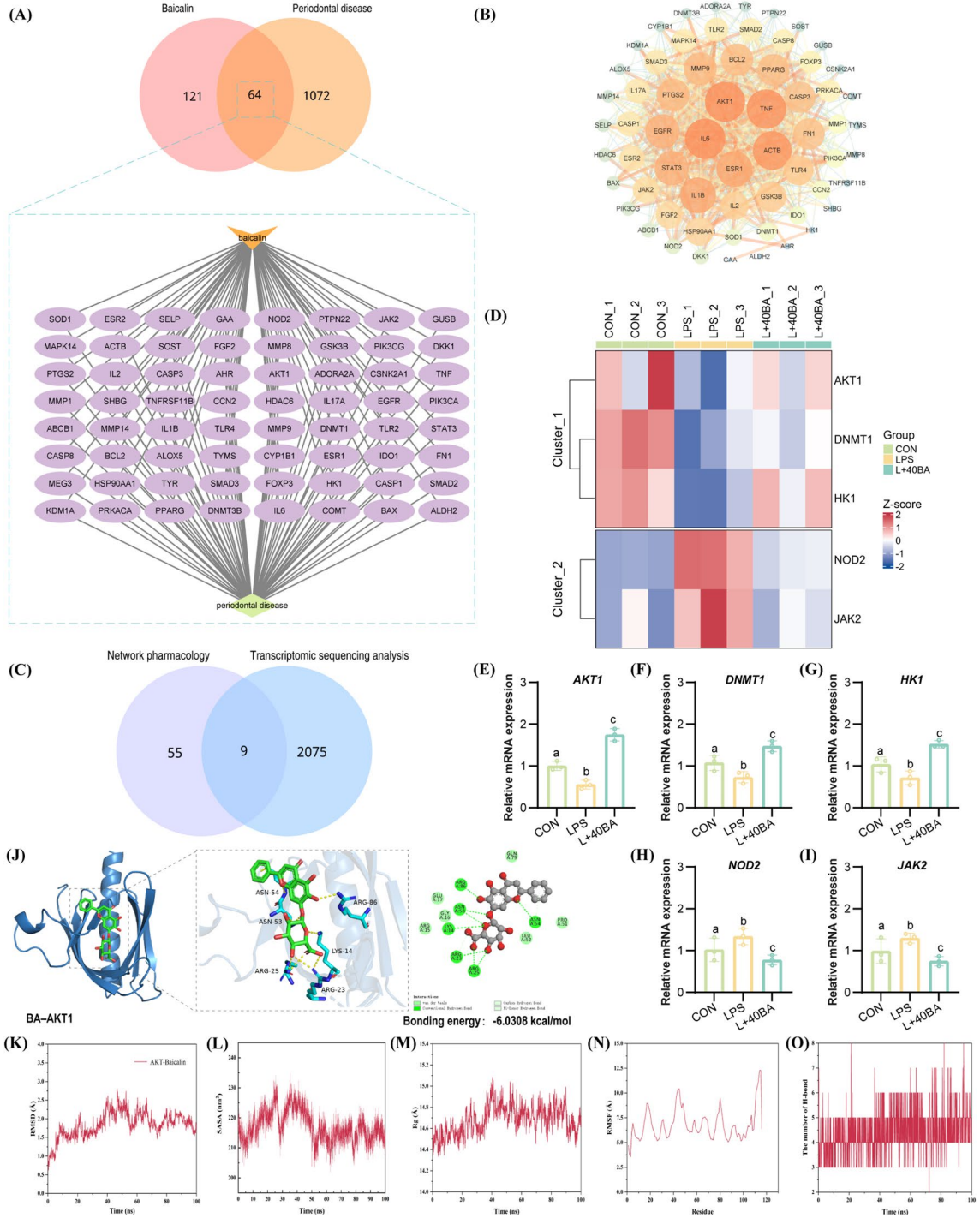

Fig. 3 Network pharmacology and RNA-Seq analysis identify AKT1 as a potential target for the treatment and prevention of periodontal disease. (**A**) Venn diagram showing the intersection analysis of common targets between BA and periodontal disease. (**B**) PPI network diagram illustrating the relationship between BA and periodontal disease targets. (**C**) Venn diagram depicting the overlap of differentially expressed mRNAs. (**D**) Heatmap of target mRNA expression in hPDLCs treated with LPS and BA. (**E**-**I**) Impact of BA on the levels of AKT1, DNMT1, HK1, NOD2, and JAK2 in LPS-treated hPDLCs for 12 h, as measured by qRT-PCR (relative to GADPH, $n = 3$). (**J**) Molecular docking results showing the interaction between AKT1 and BA. (K-O) RMSD, SASA, Rg, RMSF and Hydrogen bonding analysis of the AKT-BA complex. Statistically significant differences ($P < 0.05$) are indicated by distinct lowercase letters

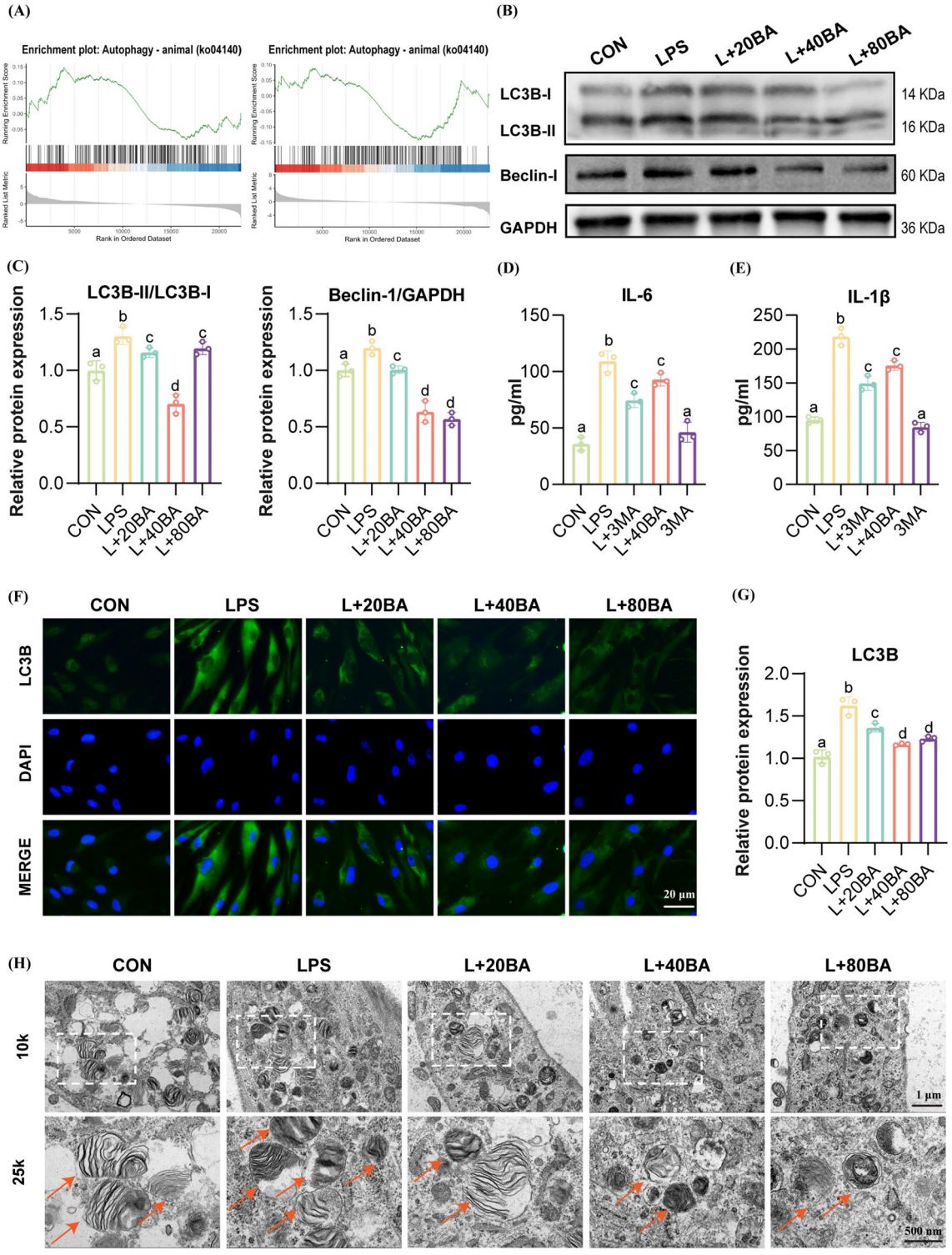

Fig. 4 BA reduces inflammatory response by inhibiting autophagy in hPDLCs. (**A**) GSEA revealing a marked enrichment of autophagy-related genes in the control, LPS, and LPS + 40BA groups ($n = 3$). (**B**) Effects of different concentrations of BA on LC3B and Beclin-1 expression in LPS-treated hPDLCs for 12 h, measured by Western blotting. ($n = 3$). (**C**) Quantitative assessment of Western blotting results presented in panel (**B**). (**D**-**E**) Effects of 3-MA on IL-6 and IL-1β secretion in the LPS-treated hPDLCs, measured using ELISA ($n = 3$). (**F**) Immunostaining of LC3B in hPDLCs after control, LPS, and different concentrations of BA and LPS treatment. (**G**) Quantitative analysis of the immunofluorescence results shown in panel (**F**). (**H**) TEM images of hPDLCs from the control, LPS, and LPS + BA groups. Statistically significant differences ($P < 0.05$) are indicated by distinct lowercase letters

and lowered the levels of LC3B-II/ LC3B-I and Beclin-1 that were elevated by LPS. Immunofluorescence staining showed higher LC3B expression in the LPS group, which was notably decreased following BA treatment (Fig. 4F). TEM further confirmed decreased autophagic activity following BA treatment (Fig. 4H). To further investigate the relationship between BA-mediated inhibition of autophagy and inflammatory responses, we co-treated BA with 3-MA. In the LPS + 3-MA group, the levels of IL-6 and IL-1β were notably lower in comparison with the LPS group (Fig. 4D-E). A comparable decrease in these proteins was detected in the LPS + 40BA group, suggesting that BA effectively inhibited the inflammatory response. These results indicate that BA notably alleviates the LPS-triggered inflammation in hPDLCs, which effects comparable to those of 3-MA. Overall, our findings suggest that BA alleviates the LPS-induced inflammatory response by inhibiting autophagy in hPDLCs.

BA inhibits hPDLCs autophagy through the activation of the PI3K/AKT/mTOR signaling pathway

KEGG enrichment analysis revealed that BA regulates autophagy in hPDLCs primarily through the MAPK, TNF and PI3K/AKT pathways, with AKT1 identified as the most significant target gene (Fig. 3). This indicated that the PI3K-AKT pathway could be the main mechanism by which BA modulates autophagy. The kinase mammalian target of rapamycin (mTOR) is a key regulator of autophagy and acts as a downstream target of the phosphatidylinositol 3-kinase (PI3K) and AKT signaling pathways [29, 30]. The PI3K/AKT/mTOR pathway is crucial for regulating various autophagy-related biological processes, including cell growth, development, and pathogen defense [29, 30]. In order to investigate the connection between BA and the PI3K/AKT/mTOR pathway, we focused on the activation of this pathway in LPS-treated hPDLCs. Both the PI3K/AKT and mTOR pathways showed significant enrichment in the LPS + 40BA group relative to the LPS group, as indicated in Fig. 5A and B. Western blotting analysis demonstrated that LPS reduced the phosphorylation of PI3K, AKT, and mTOR, while BA treatment significantly reversed these effects (Fig. 5B and C, supplementary Figure S4), with total protein levels remaining unchanged. Thus, BA positively regulated the PI3K/AKT/mTOR pathway in an inflammatory context. To better understand the involvement of this pathway, LPS-treated hPDLCs were exposed to BA following treatment with 740Y-P or LY294002. As illustrated in Fig. 5D and E (supplementary Figure S5), the higher radios of p-PI3K/PI3K, p-AKT/AKT, and p-mTOR/mTOR were observed in the 740Y-P group contrasted with LPS + 40BA group. Additionally, TEM and ELISA analyses showed a marked decrease in autophagosomes and inflammatory markers (IL-6, IL-1β) in the 740Y-P group relative to LPS + 40BA (Fig. 5F-H), while LY294002 treatment reversed these effects. Molecular docking simulations showed a binding energy of -7.1662 kcal/mol between BA and PI3Kγ, indicating a high affinity (Fig. 5I). These results indicate that BA exerts anti-inflammatory actions through activating the PI3K/AKT/mTOR pathway, which in turn inhibits autophagy.

Discussion

Periodontal disease is primarily caused by unresolved inflammation in the periodontium, with periodontitis manifesting as an exacerbated inflammatory state [31]. This disease is typically precipitated by bacterial components and antigens that trigger the production and secretion of pro-inflammatory cytokines, such as IL-4, IL-6, IL-12, IL-1β and TNF-α, in gingival tissues [2, 32]. In this research, we established LPS-induced periodontal inflammation model, characterized by significant upregulation of both mRNA and protein expression of IL-6 and IL-1β (Fig. 1D-G). Given its high prevalence, persistent inflammation, and suboptimal treatment outcomes, periodontal disease poses a considerable challenge in dental medicine [1]. This has led to increased efforts in discovering and developing novel anti-inflammatory compounds, particularly from natural sources, highlighting the growing interest in innovative therapeutic strategies.

In the present study, BA treatment significantly downregulated the mRNA and protein levels of cytokines (such as IL-6 and IL-1β) triggered by *Pg*-LPS in hPDLCs, reducing their inflammatory response (Fig. 1I-L). This is consistent with previous reports that BA has anti-inflammatory properties [11]. Our results further demonstrate that BA can target specific inflammatory mechanisms in periodontal disease, indicating its potential as a supplementary treatment. However, the specific molecular mechanism by which BA regulates these inflammatory responses remains to be further explored.

Network pharmacology and RNA-Seq analysis identified nine key targets that are likely involved in BA's action in periodontal disease treatment (Fig. 3C). Among these, AKT1 was highlighted as a significant target gene. AKT is a serine/threonine kinase and a crucial component of the PI3K/AKT/mTOR signaling pathway, which acts as a negative regulator of the autophagy process [29]. AKT1 is a key regulator of autophagy [33, 34], as confirmed by PCR experiments (Fig. 3E). In summary, AKT1 exhibited the most pronounced expression changes among the five core genes involved in BA's regulation of inflammatory response in hPLDCs. Additionally, molecular docking simulations revealed a strong binding affinity between AKT1 and BA, with minimal binding energy (Fig. 3J). This interaction was further analyzed through molecular dynamics simulations, which confirmed a stable and consistent binding of baicalin to AKT1 (Fig. 3K-O). These

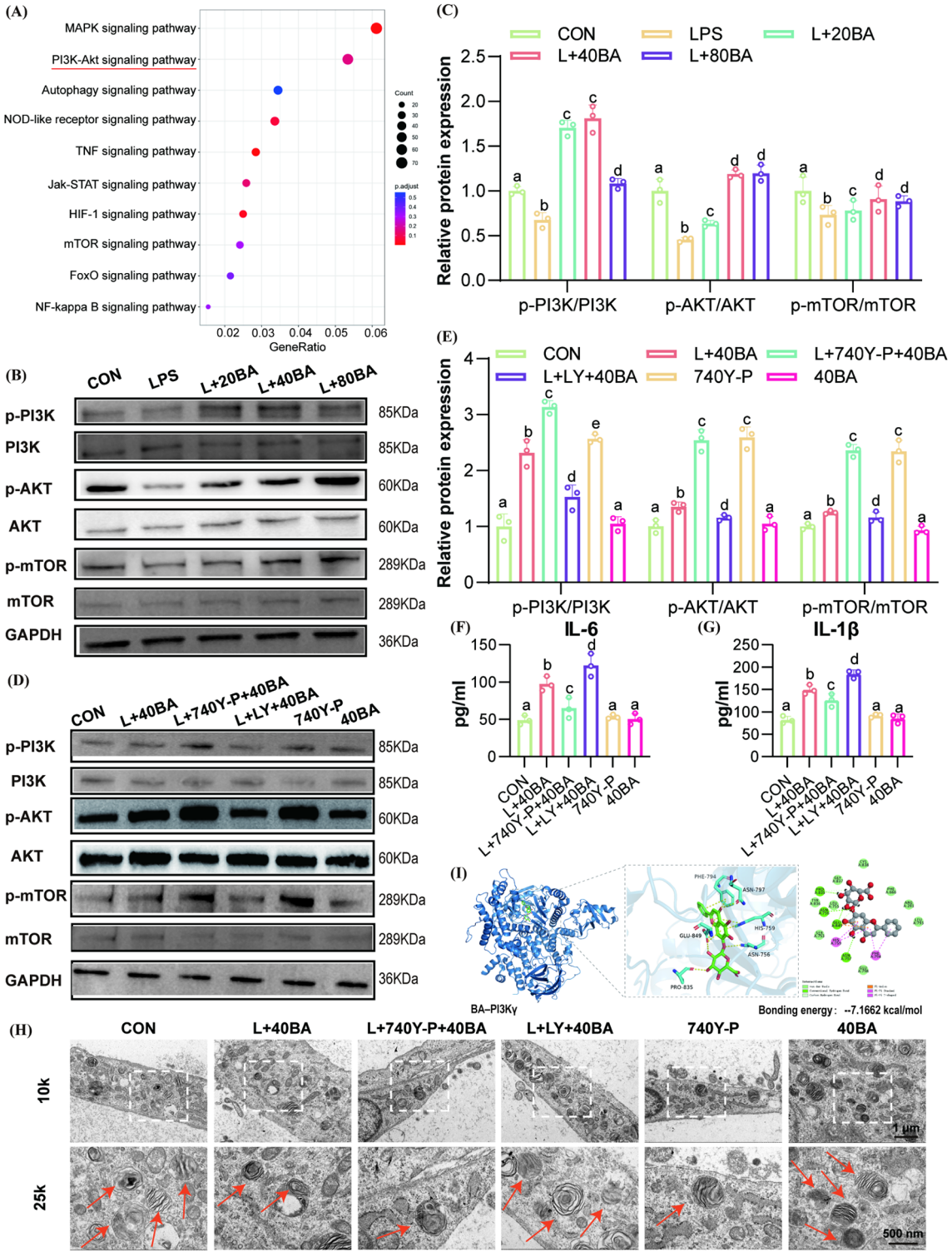

Fig. 5 BA inhibits hPDLCs autophagy through the activation of the PI3K/AKT/mTOR signaling pathway. (**A**) KEGG pathway enrichment analysis showing the pathway associated with autophagy regulation. (**B**) Western blotting analysis of pathway-related proteins expression in the control, LPS, LPS + 20BA, LPS + 40BA, and LPS + 80BA groups ($n = 3$). (**C**) Quantitative evaluation of Western blotting presented in panel (**B**). (**D**) Western blotting analysis of pathway-related proteins expression in control, LPS, LPS + 40BA, LPS + 40BA + 740Y-P, LPS + 40BA + LY, 740Y-P, and 40BA group ($n = 3$). (**E**) Quantitative evaluation of Western blotting presented in panel (**D**). (**F**-**G**) ELISA was used to measure the levels of IL-6 and IL-1β secreted in the control, LPS, LPS + 40BA, LPS + 40BA + 740Y-P, LPS + 40BA + LY, 740Y-P, and 40BA groups ($n = 3$). (**H**) Representative TEM images of hPDLCs in control, LPS, and various concentrations of BA and LPS groups. (**I**) Molecular docking results showing the binding between PI3Kγ and BA. Statistically significant differences ($P < 0.05$) are indicated by distinct lowercase letters

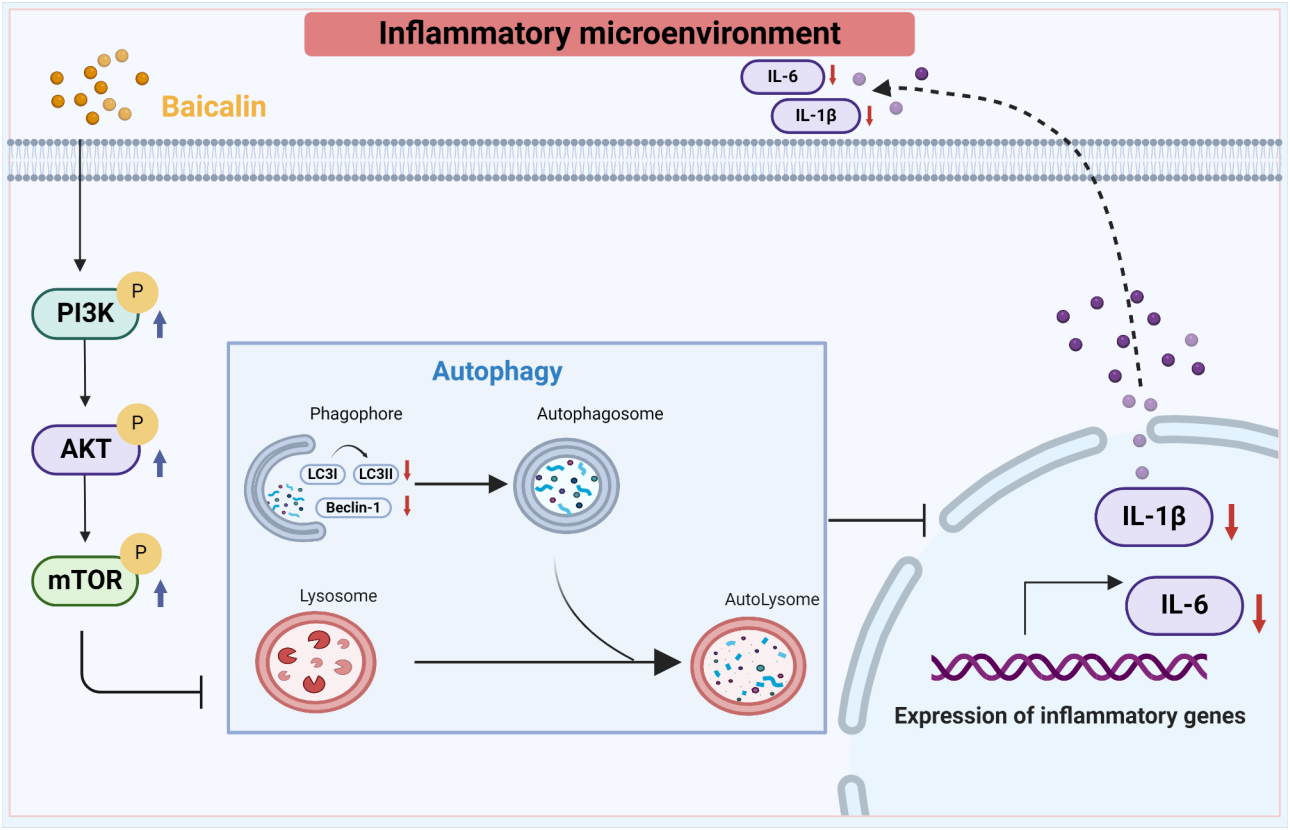

Fig. 6 Illustration of the proposed mechanism of BA in treating LPS-induced periodontal disease. BA inhibits the autophagy process in periodontal cells by promoting the phosphorylation of PI3K, AKT, and mTOR. This signaling cascade resulted in a reduction of autophagy-related proteins, specifically LC3B-II and Beclin-1, ultimately suppressing the secretion of IL-6 and IL-1β proteins (created with BioRender.com)

results directly show the key role of AKT1 in BA's regulation of periodontal - related processes in hPDLCs.

This study elucidated that BA alleviated the inflammatory response in hPDLCs by inhibiting autophagy. LPS treatment significantly enhanced the levels of autophagy-related genes, an effect that was effectively reversed by BA. Specifically, BA downregulated the protein levels of LC3BII/I and Beclin-1/GAPDH, reduced LC3B protein staining, and diminished the number of autophagosomes. Notably, the autophagy inhibitor 3-MA also attenuated the inflammatory response in hPDLCs, indicating that both BA and 3-MA inhibit autophagy and subsequently downregulate pro-inflammatory markers like IL-6 and IL-1β. These results imply that BA could be a potential therapeutic approach for reducing inflammation in periodontal disease by inhibiting autophagy. Similar conclusions have been drawn in other cell types, reinforcing the generalizability of BA's effects. For instance, BA has been shown to counteract LPS-induced autophagy downregulation in HT-29 intestinal epithelial cells while suppressing NF-κB activation and restoring claudin-1 expression [35]. This dual action indicates that BA modulates both autophagy and inflammatory pathways in response to stimuli, consistent with our observations in hPDLCs.

In our study, BA regulated autophagy in hPDLCs through the PI3K/AKT/mTOR pathway. The PI3K/AKT/mTOR pathway plays a central role in regulating autophagy [6]. Our study observed reduced phosphorylation of PI3K, AKT, and mTOR in hPDLCs exposed to *Pg*-LPS, while BA treatment significantly reversed these changes, enhancing phosphorylation at the PI3K try458 site, which activated AKT (Fig. 5B-E). This activation stimulated mTORC1 at Ser2448, leading to increased autophagy. These results in hPDLCs highlight BA's role in modulating the PI3K/AKT/mTOR pathway to regulate autophagy and inflammation, providing evidence for its potential as a therapeutic agent in periodontal disease treatment.

The PI3K/AKT/mTOR pathway plays a central role in regulating autophagy [6]. A number of studies have indicated that BA targets PI3K/AKT and mTOR signaling [36–38], consistent with our finding in Fig. 5A. We also explored how BA influence hPDLCs' autophagy through this pathway (Fig. 2). Our study observed reduced phosphorylation of PI3K, AKT, and mTOR in hPDLCs exposed to *Pg*-LPS, while BA treatment significantly reversed these changes, enhancing phosphorylation at the PI3K try458 site, which activated AKT (Fig. 5B-E). This activation stimulated mTORC1 at Ser2448, leading

to increased autophagy. 740Y-P, a PI3K/AKT agonist, nullified BA's effects on autophagy and inflammation, while LY294002 enhanced these effects (Fig. 5H). BA activates the PI3K/AKT pathway to exert protective effects in different injury contexts. This includes enhancing recovery by reducing apoptosis in spinal cord injury and protecting against brain damage in hypoxic-ischemic conditions in neonates [39, 40]. Conversely, it promotes autophagy and reduces inflammation in *Mycobacterium tuberculosis* (*M. tuberculosis*)- infected cells by inhibiting this pathway [41]. These actions highlight BA's dual regulatory role in modulating the PI3K/AKT/mTOR signaling, which varies by disease context and demonstrates its therapeutic potential.

In summary, our research demonstrated that BA suppressed inflammation in hPDLCs by modulating autophagy through the PI3K/AKT/mTOR pathway (Fig. 6). The molecular docking results further confirmed a strong interaction between PI3K and BA (Fig. 5I). These results highlight the promise of BA in treating periodontal disease, suggesting the need for further investigation into its clinical applications.

However, this study has some limitations. Although our in vitro experiments confirmed the specific signaling pathway through which BA regulates autophagy in hPDLCs, further validation using appropriate in vivo models is necessary to better mimic the complex periodontal environment. Rodent models, such as ligature-induced periodontitis in rats or mice, provide a well-established system to evaluate periodontal inflammation and bone loss while allowing molecular and histological assessments of BA's effects. However, considering anatomical and physiological differences between rodent and human periodontium, larger animal models, such as canine periodontitis models, are preferable for assessing clinical translational potential since they share greater similarities in periodontal structure, microbiota composition, and disease progression with humans. Future studies should integrate both rodent models for mechanistic validation and large-animal models for clinical feasibility assessment to comprehensively evaluate BA's therapeutic potential.

Conclusion

This study confirmed that 40 μM BA effectively attenuates LPS-induced periodontal inflammation in hPDLCs by inhibiting autophagy, highlighting its potential as a therapeutic agent for periodontal disease. Among the tested concentrations, 40 μM BA exhibited the most significant anti-inflammatory and autophagy-suppressing effects, justifying its selection for further validation. These findings not only elucidate the mechanism by which BA modulates periodontal inflammation but also suggest its broader potential in managing inflammatory diseases. However, further studies, including in vivo and clinical investigations, are necessary to confirm these effects and explore the optimal dosing strategies for therapeutic applications.

List of Abbreviations

3-MA	3-Methyladenine
aGVHD	Acute Graft-versus-host disease
AR	Allergic rhinitis
BA	Baicalin
CCK-8	Cell Counting Kit-8
ELISA	Enzyme-linked immunosorbent assay
HGFs	Human gingival fibroblasts
IL-1β	Interleukin-1β
IL-6	Interleukin-6
IL-88	Interleukin-
LPS	Lipopolysaccharide
mTOR	Mammalian target of rapamycin
MMP-1	Matrix metalloproteinase-1
MMP-8	Matrix metalloproteinase-8
M. tuberculosis	*Mycobacterium tuberculosis*
M. gallisepticum	*Mycoplasma gallisepticum*
OA	Osteoarthritis
PDLCs	Periodontal ligament cells
PI3K	Phosphatidylinositol 3 kinase
PMNs	Polymorphonuclear neutrophils
P.gingivalis	*Porphyromonas gingivalis*
PPI	Protein-protein interaction
qRT-PCR	Quantitative real-time PCR
ROS	Reactive oxygen species
RA	Rheumatoid arthritis
RNA-Seq	RNA sequencing
SE	Status epilepticus
TTM	Tetrathiomolybdate
TEM	Transmission electron microscopy
TNF-α	Tumour necrosis factor alpha

Supplementary Information

The online version contains supplementary material available at https://doi.org/10.1186/s12903-025-05913-7.

Supplementary Material 1

Acknowledgements

All authors are grateful for the technical assistance from the Experimental Medicine Center, Tongji Hospital, Tongji Medical College, Huazhong University of Science and Technology. All authors would like to thank for excellent technical assistance from Biorender platform (https://www.biorender.com/). We thank Shanghai Tengyun Biotechnology Co., Ltd. for developing Hiplot Pro platform (https://hiplot.com.cn/) and providing technical assistance and valuable tools for data analysis and visualization.

Author contributions

Guangxun Zhu was instrumental in formulating the concept, devising the methodology, and overseeing the project's design, in addition to contributing to the manuscript's composition and revision. Yan Liu contributed to data collection and analysis, as well as drafting and critically revising the manuscript. Jing Mao executed the investigation and provided oversight. Ming Jiang oversaw the project and managed its administration. Xu Qin was at the helm of the research design. Yifan Cheng played a pivotal role in conducting the in vitro experiments and drafting the manuscript. All authors approved the final version of the manuscript.

Funding

This work was supported by the Natural Science Foundation of Hubei Province (2021CFB056, 2019CFB688, 2023AFB653, 2023AFB765) and National Natural Science Foundation of China (81800981).

Data availability
The RNA transcriptome sequencing data generated and analyzed during the current study are available in the NCBI repository under the accession number PRJNA1211272.

Declarations

Ethics approval and consent to participate
The study strictly adhered to the ethical principles of the Declaration of Helsinki. The protocol was approved by the Ethics Committee of Tongji Hospital Ethics Committee (TJ-IRB202502011). Informed consent was obtained from all individual participants included in the study.

Consent for publication
Not applicable.

Competing interests
The authors declare no competing interests.

Declaration of competing interest
The authors indicate no potential conflicts of interest.

ORCID
Yan Liu: 0000-0002-8193-6729.
Guangxun Zhu: 0000-0002-8705-2908.

Author details
[1]Department of Stomatology, Tongji Hospital, Tongji Medical College, Huazhong University of Science and Technology, Wuhan 430030, China
[2]School of Stomatology, Tongji Medical College, Huazhong University of Science and Technology, Wuhan 430030, China
[3]Hubei Province Key Laboratory of Oral and Maxillofacial Development and Regeneration Wuhan, 430030 Hubei, China
[4]Central Laboratory, Peking University School and Hospital for Stomatology & National Center for Stomatology & National Clinical Research Center for Oral Diseases & National Engineering Research Center of Oral Biomaterials and Digital Medical Devices & Beijing Key Laboratory of Digital Stomatology & Research Center of Engineering and Technology for Computerized Dentistry Ministry of Health & NMPA Key Laboratory for Dental Materials & National Engineering Research Center of Oral Biomaterials and Digital Medical Devices, Beijing 100081, China

Received: 18 January 2025 / Accepted: 31 March 2025
Published online: 10 April 2025

References

1. Kinane DF, Stathopoulou PG, Papapanou PN. Periodontal diseases. Nat Reviews Disease Primers. 2017;3:17038.
2. Kinane DF. Causation and pathogenesis of periodontal disease. Periodontol 2000. 2001;25:8–20.
3. Deretic V, Saitoh T, Akira S. Autophagy in infection, inflammation and immunity. Nat Rev Immunol. 2013;13(10):722–37.
4. El-Awady AR, Arce RM, Cutler CW. Dendritic cells: microbial clearance via autophagy and potential Immunobiological consequences for periodontal disease. Periodontol 2000. 2015;69(1):160–80.
5. Jiang M, Li Z, Zhu G. The role of autophagy in the pathogenesis of periodontal disease. Oral Dis. 2020;26(2):259–69.
6. Kim WJ, Park SY, Kim OS, Park HS, Jung JY. Autophagy upregulates inflammatory cytokines in gingival tissue of patients with periodontitis and lipopolysaccharide-stimulated human gingival fibroblasts. J Periodontol. 2022;93(3):380–91.
7. Zhao Z, Ming Y, Li X, Tan H, He X, Yang L, Song J, Zheng L. Hyperglycemia aggravates periodontitis via autophagy impairment and ROS-Inflammasome-Mediated macrophage pyroptosis. Int J Mol Sci 2023, 24(7).
8. Xiao J, Huang X, Wang H, Peng Y, Liu H, Huang H, Ma L, Wang C, Wang X, Cao Z. CKIP-1 promotes P. gingivalis-Induced inflammation of periodontal soft tissues by inhibiting autophagy. Inflammation. 2023;46(5):1997–2010.
9. Jang JS, Hong SJ, Mo S, Kim MK, Kim YG, Lee Y, Kim HH. PINK1 restrains periodontitis-induced bone loss by preventing osteoclast mitophagy impairment. Redox Biol. 2024;69:103023.
10. Zhang L, Tsai IC, Ni Z, Chen B, Zhang S, Cai L, Xu Q. Copper chelation therapy attenuates periodontitis inflammation through the cuproptosis/autophagy/lysosome axis. Int J Mol Sci 2024, 25(11).
11. Guo LT, Wang SQ, Su J, Xu LX, Ji ZY, Zhang RY, Zhao QW, Ma ZQ, Deng XY, Ma SP. Baicalin ameliorates neuroinflammation-induced depressive-like behavior through Inhibition of toll-like receptor 4 expression via the PI3K/AKT/FoxO1 pathway. J Neuroinflamm. 2019;16(1):95.
12. Cao Z, Li C, Zhu G. Inhibitory effects of Baicalin on IL-1beta- induced MMP-1/TIMP-1 and its stimulated effect on collagen-I production in human periodontal ligament cells. Eur J Pharmacol. 2010;641(1):1–6.
13. Zhu G, Li C, Cao Z. Inhibitory effect of flavonoid Baicalin on degranulation of human polymorphonuclear leukocytes induced by interleukin-8: potential role in periodontal diseases. J Ethnopharmacol. 2007;109(2):325–30.
14. Ming J, Zhuoneng L, Guangxun Z. Protective role of flavonoid Baicalin from scutellaria baicalensis in periodontal disease pathogenesis: A literature review. Complement Ther Med. 2018;38:11–8.
15. Cheng Y, Yan M, He S, Xie Y, Wei L, Xuan B, Shang Z, Wu M, Zheng H, Chen Y, et al. Baicalin alleviates angiotensin II-induced cardiomyocyte apoptosis and autophagy and modulates the AMPK/mTOR pathway. J Cell Mol Med. 2024;28(9):e18321.
16. Sun X, Pisano M, Xu L, Sun F, Xu J, Zheng W, Liu X, Zhang Y, Sun R, Cui X. Baicalin regulates autophagy to interfere with small intestinal acute graft-versus-host disease. Sci Rep. 2022;12(1):6551.
17. Yang B, Wen HY, Liang RS, Lu TM, Zhu ZY, Wang CH. Hippocampus protection from apoptosis by Baicalin in a LiCl-pilocarpine-induced rat status epilepticus model through autophagy activation. World J Psychiatry. 2023;13(9):620–9.
18. Wang G, Liang J, Gao LR, Si ZP, Zhang XT, Liang G, Yan Y, Li K, Cheng X, Bao Y, et al. Baicalin administration attenuates hyperglycemia-induced malformation of cardiovascular system. Cell Death Dis. 2018;9(2):234.
19. Zhu HY, Han L, Shi XL, Wang BL, Huang H, Wang X, Chen DF, Ju DW, Feng MQ. Baicalin inhibits autophagy induced by influenza A virus H3N2. Antiviral Res. 2015;113:62–70.
20. Ishfaq M, Wu Z, Wang J, Li R, Chen C, Li J. Baicalin alleviates Mycoplasma gallisepticum-induced oxidative stress and inflammation via modulating NLRP3 inflammasome-autophagy pathway. Int Immunopharmacol. 2021;101(Pt B):108250.
21. Chen X, Wang Y, Cai J, Wang S, Cheng Z, Zhang Z, Zhang C. Anti-inflammatory effect of Baicalin in rats with adjuvant arthritis and its autophagy-related mechanism. Technol Health Care: Official J Eur Soc Eng Med. 2022;30(S1):191–200.
22. Li J, Lin X, Liu X, Ma Z, Li Y. Baicalin regulates Treg/Th17 cell imbalance by inhibiting autophagy in allergic rhinitis. Mol Immunol. 2020;125:162–71.
23. Li Z, Cheng J, Liu J. Baicalin protects human OA chondrocytes against IL-1β-Induced apoptosis and ECM degradation by activating autophagy via MiR-766-3p/AIFM1 axis. Drug Des Devel Ther. 2020;14:2645–55.
24. Hang Y, Qin X, Ren T, Cao J. Baicalin reduces blood lipids and inflammation in patients with coronary artery disease and rheumatoid arthritis: a randomized, double-blind, placebo-controlled trial. Lipids Health Dis. 2018;17(1):146.
25. Orzechowska B, Chaber R, Wiśniewska A, Pajtasz-Piasecka E, Jatczak B, Siemieniec I, Gulanowski B, Chybicka A, Błach-Olszewska Z. Baicalin from the extract of scutellaria baicalensis affects the innate immunity and apoptosis in leukocytes of children with acute lymphocytic leukemia. Int Immunopharmacol. 2014;23(2):558–67.
26. Ma N, Pan B, Ge L, Li M, Zhu H, Deng X, Li D, Wang X, Wu L, Xiao J, et al. Efficacy and safety of Tanreqing injection for cough caused by acute tracheobronchitis disease: A systematic review and meta-analysis of randomized controlled trials. J Ethnopharmacol. 2024;321:117429.
27. Isola G, Matarese M, Ramaglia L, Iorio-Siciliano V, Cordasco G, Matarese G. Efficacy of a drug composed of herbal extracts on postoperative discomfort after surgical removal of impacted mandibular third molar: a randomized, triple-blind, controlled clinical trial. Clin Oral Invest. 2019;23(5):2443–53.
28. Isola G, Polizzi A, Iorio-Siciliano V, Alibrandi A, Ramaglia L, Leonardi R. Effectiveness of a nutraceutical agent in the non-surgical periodontal therapy: a randomized, controlled clinical trial. Clin Oral Invest. 2021;25(3):1035–45.
29. Hou X, Hu Z, Xu H, Xu J, Zhang S, Zhong Y, He X, Wang N. Advanced glycation endproducts trigger autophagy in cadiomyocyte via RAGE/PI3K/AKT/mTOR pathway. Cardiovasc Diabetol. 2014;13:78.
30. Ravanan P, Srikumar IF, Talwar P. Autophagy: the spotlight for cellular stress responses. Life Sci. 2017;188:53–67.

31. Pihlstrom BL, Michalowicz BS, Johnson NW. Periodontal diseases. Lancet (London England). 2005;366(9499):1809–20.
32. Marchesan JT. Inflammasomes as contributors to periodontal disease. J Periodontol. 2020;91(Suppl 1):S6–11.
33. Cheng B, Li T, Li F. Study on the multitarget mechanism of alliin activating autophagy based on network Pharmacology and molecular Docking. J Cell Mol Med. 2022;26(22):5590–601.
34. Chen X, Han K, Lin G, Liu C, Wang S, Shi X, Hu Z, Wu C, Xu X, Hu C. Ctenopharyngodon Idella STAT3 alleviates autophagy by up-regulating BCL-2 expression. Fish Shellfish Immunol. 2019;91:194–201.
35. Rizzo V, Ferlazzo N, Currò M, Isola G, Matarese M, Bertuccio MP, Caccamo D, Matarese G, Ientile R. Baicalin-Induced autophagy preserved LPS-Stimulated intestinal cells from inflammation and alterations of paracellular permeability. Int J Mol Sci 2021, 22(5).
36. Huang Y, Hu J, Zheng J, Li J, Wei T, Zheng Z, Chen Y. Down-regulation of the PI3K/Akt signaling pathway and induction of apoptosis in CA46 Burkitt lymphoma cells by Baicalin. J Experimental Clin cancer Research: CR. 2012;31(1):48.
37. Pang H, Wu T, Peng Z, Tan Q, Peng X, Zhan Z, Song L, Wei B. Baicalin induces apoptosis and autophagy in human osteosarcoma cells by increasing ROS to inhibit PI3K/Akt/mTOR, ERK1/2 and β-catenin signaling pathways. J Bone Oncol. 2022;33:100415.
38. Zhao H, Li C, Li L, Liu J, Gao Y, Mu K, Chen D, Lu A, Ren Y, Li Z. Baicalin alleviates bleomycin–induced pulmonary fibrosis and fibroblast proliferation in rats via the PI3K/AKT signaling pathway. Mol Med Rep. 2020;21(6):2321–34.
39. Zhao R, Wu X, Bi XY, Yang H, Zhang Q. Baicalin attenuates blood-spinal cord barrier disruption and apoptosis through PI3K/Akt signaling pathway after spinal cord injury. Neural Regeneration Res. 2022;17(5):1080–7.
40. Zhou ZQ, Li YL, Ao ZB, Wen ZL, Chen QW, Huang ZG, Xiao B, Yan XH. Baicalin protects neonatal rat brains against hypoxic-ischemic injury by upregulating glutamate transporter 1 via the phosphoinositide 3-kinase/protein kinase B signaling pathway. Neural Regeneration Res. 2017;12(10):1625–31.
41. Zhang Q, Sun J, Wang Y, He W, Wang L, Zheng Y, Wu J, Zhang Y, Jiang X. Antimycobacterial and Anti-inflammatory mechanisms of Baicalin via induced autophagy in macrophages infected with Mycobacterium tuberculosis. Front Microbiol. 2017;8:2142.

Publisher's note